Journal of Hydrosciences and Environment
ISSN: 2345-5608

Numerical Study of Hydraulic Flow and Determining the Equations Governing Separation Zones in Intakes

S. Karimi [1], H. Bonakdari [1, *]

1, Plant Protection Department, Faculty of Agriculture, University of Tabriz, Tabriz, Iran

ARTICLEINFO

Article history:

Received:12 March 2023
Accepted: 18 April 2023

Keywords:
intake
separation zone
ANSYS-CFX model
k-ω turbulence model

ABSTRACT

Intakes are used in rives and channels to control and deviate the flow. The deviation in the intake leads to the formation of a complex flow in the branch channel mouth therefore being familiar with the hydraulic flow in intakes is of great importance. The experimental model was simulated using ANSYS-CFX software in this study. Numerical modeling was carried out in a three- dimensional manner based on k-ω turbulence model. The verification results indicate that the results of the numerical model correspond fairly well to the results of the experimental model with a relative error value (MAPE) of 5%. After verifying the CFX model in this research the effects of different parameters such as discharge ratio, different width ratios, Froude number of the incoming flow, and intake angle were studies on the size of the separation come. According to the obtained numerical results, proper formulas have been developed for anticipating the effects of these parameters on separation zone.

1. Introduction

Intakes are among hydraulic structures used for the purposes of controlling and diverting the flow in irrigation networks and agriculture. Determining the flow pattern from the main channel to the branch channel is of crucial importance in these hydraulic structures. A part of the flow deviates from the main channel and enters the branch channel when dewatering the river due to suction force and leads to the formation of an area called the separation zone near the mouth of the branch channel [1, 2]. The longitudinal velocity of the flow

Law and Reynolds [7] carried out an analytical and experimental study on deviation and main channels and presented an equation for discharge ratios along with the Froude number before and after the cross section and the width ratios of the two channels. Neary and Odgaard [8] conducted experimental studies on flow pattern, flow separation line, stagnation zone and separation zone in 90° intakes. They concluded that rotating flow's strength increases in the separation zone as the ratio of the velocity in the intake channel to the main channel increases. The stagnation zone is also formed adjacent to the upstream side within the intake channel in which sedimentation occurs.

Ramamurthy et al.'s [9] experimental model was three-dimensionally simulated through using ANSYS-CFX software in order to study hydraulic flow in this study. After verifying the results ofthe numerical model, the effects of different influential parameters such as the effect of the distributed discharge ratio, different width ratios, incoming flow Froude number and intake angle were studied numerically on the size of the separation zone and some Equations will also be presented numerically.

*Corresponding author's email:Sohrab_karimi68@yahoo.com

2.Materials and Methods

2.1. Experimental model

Ramamurthy et al.'s [9] experimental results were used in this study in order to verify the results of the numerical model. Ramamurthy et al.'s [9] experimental model includes a rectangular channel attached to an intake with a 90- degree angle. Both channels lack longitudinal slope. The lengths of the main channel and the branch channel are 6.198 meters and 2.794 meters respectively the widths of the channels are the same and equal to 0.61 meters and they are 0.305 meters high (Figure 1). The branch channel is located 2.794 meters away from the main channel's entrance. The discharge in the entrance of the main channel is Q_u = 0.046 m^3/s and Q_b = 0.038 m^3/s in the branch channel. The ratio of the branch channel to the main channel is equal to Qr = Qb / Qu= 0.838.

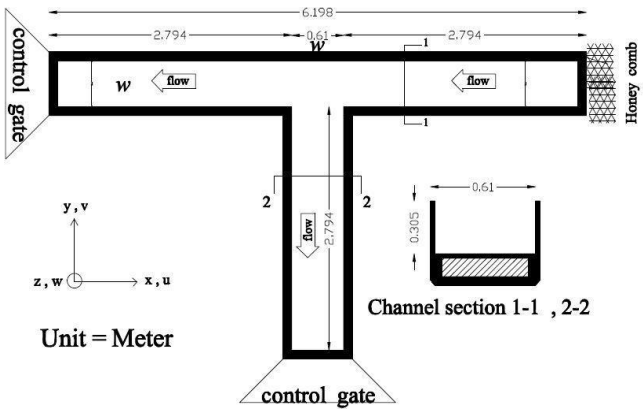

Fig. 1. Ramamurthy et al.'s [9] experimental channel plan

2.2. Numerical model

In ANSYS-CFX software we use Navier- Stokes continuity equation and mean equation in order to solve unidentifiable fluid flow field

$$\frac{\partial \rho}{\partial t}+\frac{\partial \rho U}{\partial x}+\frac{\partial \rho V}{\partial v}+\frac{\partial \rho W}{\partial z}=0 \rightarrow \frac{\partial \rho}{\partial t}+\mathrm{div}(\rho U)=0 \quad (1)$$

$$\frac{\partial}{\partial x}\left(\rho u_j\right)+\frac{\partial}{\partial x_j}\left(\rho u_i u_j\right)=\frac{\partial P}{\partial x_i}+\frac{\partial}{\partial x_j}\ \mu\ \frac{\partial u_i}{\partial x_j}+\frac{\partial u_j}{\partial x_i}\ \frac{2}{3}\delta_{ij}\frac{\partial u_i}{\partial x_j}+\frac{\partial}{\partial x_i}\left(\ \rho\overline{u_i'}\overline{u_j'}\right) \quad (2)$$

In this equation ui presents velocity in the direction of x axis and uj is velocity in the y axis direction, p is the total pressure and p is the fluid density δ_{ij} is Kronecher delta. u_iu_j represent the components of the

Reynolds stress tensor. k-ω turbulence model is used in this numerical simulation. The k-ω turbulence model is a second-degree equation. This turbulence models consists of two turbulence parameters which include kinetic energy turbulence (k) and Specific Dissipation Rate (ω) [10, 11].

Also, the two-phase volume of fluid (VOF) model has been used in order to solve air-water two- phase field to determine the changes of water level within the field. The flow is two-phase in free-surface common flows like the one in this study; in this sort of flow air phase is separated from the lower phase, meaning water, through the free surface. The barrier conditions applied to the numerical model are selected in a way to conform to the physical conditions of Ramamurthy et al.'s [9] experimental model. Therefore, Velocity inlet has been used in the main channel entrance and velocity outlet has been used for the intake exit and the exit of the main channel in order to define boundary conditions in CFX. Smooth with no slip conditions have been used for the channel walls and floor and opening boundary condition has been used for the upper surface of the channels. The definition of free surface of the flow in the dividing flow is based on eulerian viewpoint and the volume of fluid (VOF) model is used for simulating free surface changes [10-14].

One parameter that is responsible for increasing the numerical model's accuracy is proper gridding of the flow field. The main channel has been divided into three sections in order to achieve this gridding in the constructed CFX model. Its first part is 2.794 m long and located in the main channel upstream, its second section is 0.61 m long in the middle of the main channel, and its third part is 2.794 m long located in the main channel downstream. The size of the cells is 1× 0.5× 0.5 cm in the main channel upstream and downstream, 0.5× 0.5 × 0.5 cm in the middle section and the size of the network cells in the branch channel has been determined 0.5× 0.5 × 0.5 cm. Figure 2 shows the gridding of the computational field within a 90° intake.

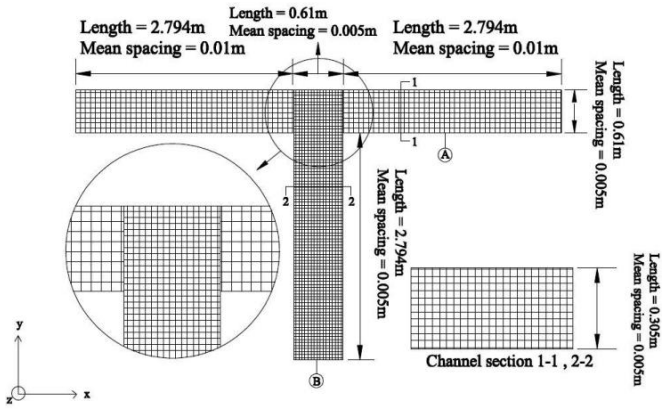

Fig. 2. Gridding the flow field through ANSYS- CFX

2.3. Verification

In order to study the accuracy of the numerical model, the results from the numerical simulation were compared with the experimental results. Dimensionless profiles of the longitudinal velocity $v^* = v/v_c$ of the numerical model and the experimental model were compared with each other in the branch channel. v* indicates the dimensionless longitudinal velocity in the branch channel and it is directed in y* direction (Figure 3). This comparison was carried out for the discharge ratio of Qr = Qb / Qu= 0.838. The dimensionless longitudinal velocities were evaluated in three cross sections of y*= -0.29, -1.0 and -0.62 within the branch channel. In Figure 3 the amounts of x, y, and z have become dimensionless with regard to the main channel's width of b= 0.61 m. two statistical indexes were used in order to study the accuracy of the modeled CFD in a manner that the results obtained from the CFD model are based on the root mean square error (RMSE) and mean absolute percentage error (MAPE) as defined in the following forms.

$$MAPE = \frac{1}{n}\sum_{i=1}^{n}\frac{\left|v_{EXP_i} - v_{CFD_i}\right|}{v_{EXP_i}} \times 100 \quad (3)$$

$$RMSE = \sqrt{\frac{1}{n}\sum_{i=1}^{n}\left(v_{EXP_i} - v_{CFD_i}\right)^2} \quad (4)$$

Where V_{EXPi} denotes the experimental velocity and V_{CFDi} denotes the velocity results of CFD model a, respectively. MAPE index indicates the difference between experimental and CFD model in the form of percentage of real values and RMSE index considers weight of larger errors by powering the difference between experimental and CFD model values.

Table 1 shows the statistical indexes between the results obtained from the CFD model and the experimental model in different cross sections of Y*.

Table 1. Statistical Indexes

	Y*= -0.29	Y*= -1.0	Y*= -1.62
RMSE	0.01	0.012	0.017
MAPE (%)	2.0	5.2	6.95

Considering table 1 the relative error average of MAPE the results of CFD model in three cross section of Y*= -0.29, -1.0, -0.62 are approximately 2%, 5.2% and 6.95% respectively which indicates a good conformity between the results of the CFD model and the experimental model. Also the amount of RMSE for three cross sections Y*= -0.29, -1.0, -0.62 is 0.01, 0.012 and 0.017 respectively (Table 1). As it could be observed in figure 3 and table 1 in the branch channel downstream y*= -1.0 and y*= -1.62 there is a small difference between the results of the numerical model and the results of the experimental model but despite that the maximum error of MAPE is equal to 6.95%. the reason for this difference is the existence of separation zone and contraction zone since due to the existence of the recirculation zone the longitudinal velocity decreases in the separation zone and the velocities turn negative. In the contraction zone and in the depth of z*= 0.0 to z*= 0.2 the velocities are at maximum level Vmax and the density of the contraction zone is more than the flow surface.

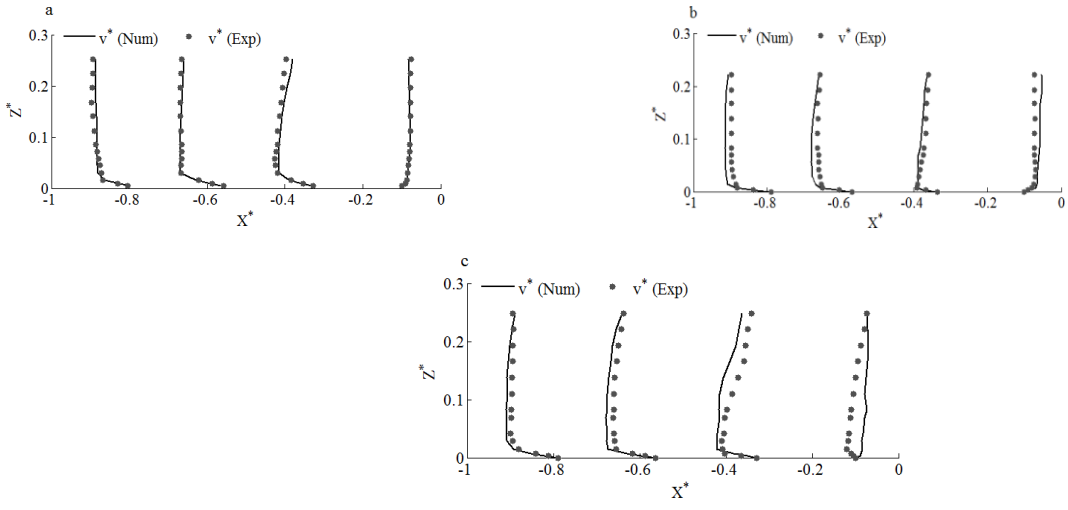

Fig 3. Verification graphs between the results of the CFX model and the Ramamurthy et al.'s [9] experimental model in: a) y*=-0.29, b) y*=-1.00 and c) y*=-1.62

x*=y*=z* are the dimensionless axial points of x, y, and z respectively. U, v, and w are the velocity aspects in x, y, and z axial points respectively. The presented velocities have become dimensionless with regard to the critical velocity in the upstream of the main channel. The critical velocity is calculated through Vc in the upstream of the main channel.

3. Studying and result

The number of the variables affecting the formation of the separation zone is extracted through the following dimensionless Equation in this study.

$$\frac{L_r}{b}, \frac{W_r}{b} = F(R, Fr, \theta, \frac{b}{B}) \qquad (5)$$

In this formula Lr/b and Wr/b are the dimensionless length and width of the separation zone respectively, R is the discharge ratio of dewatering, Fr represents the Froude number of the entering flow, θ is the intake angle and b/B is the ratio of the width of the intake to the width of the main channel.

3.1. Investigating the effect of the ratio of discharge distribution and the ratio of width to the size of the separation zone of the flow

The effect of the ratio of different widths (b/B) 1 and 2 and the ratio of discharge distribution (R) 0.32 to 0.81 for a constant Froude number of entrance flow (fr) 0.2 on length (Lr) and width (Wr) of the separation zone created in the intake is numerically studied in Figure 4 in this section.

Considering Figure 4 it could be found that an increase in the ratio of the intake channel width to the main channel, increases the length and width of the separation zone within the intake and one of the main reasons could be the stability of the entering flow while the width of the intake is increasing. The changes of Lr/b and Wr/b with regard to R in b/B=1 are also compared in Figure 5 with the experimental results of Kasthuri and Pundarikanthan [14] which have a different geometrics from the geometry of the experimental channel of Ramamurthy et al., [9]. Kasthuri and Pundarikanthan [14] measured the flow depth and the velocity foeld within the main and branch channels under subcritical flow conditions. The amounts of Wr/b and Lr/b are shown in Figure 6 with regard to different width ratios 0.5, 1, 1.5, and 2 and for 0.011 cubic meters per second constant entering discharge and for discharge distribution ratios of 0.32, 0.52 and 0.81.

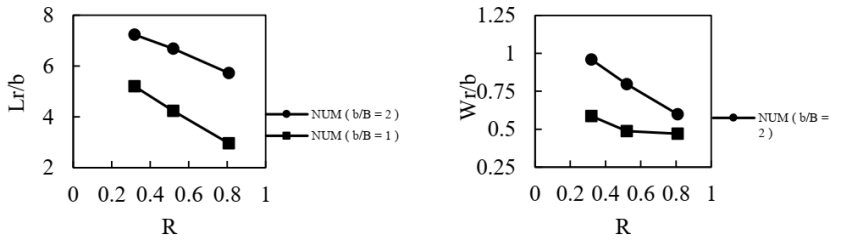

Fig 4. comparing Lr/b and Wr/b based on different Rs in different width ratios

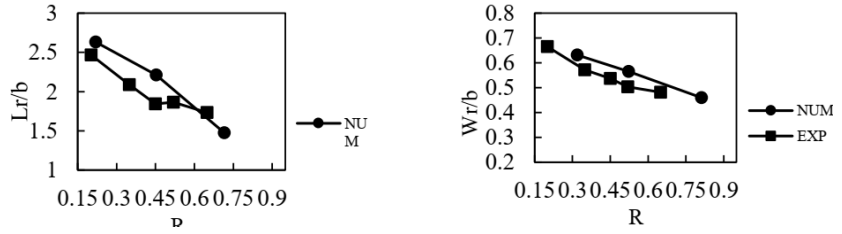

Fig 5. comparing Wr/b and Lr/b based on R in the present research with other researchers

Figure 6 indicates that for a constant discharge entering the main channel, as b/B increases, Lr/b and Wr/b increase in most cases as well, R increases in all cases and the increase in the size of the separation zone will be observable. Based on Equation 5, Equation 6 can be obtained through deleting θ and Fr since they are constant in the present research.

$$\frac{L_r}{b}, \frac{W_r}{b} = F(R, \frac{b}{B}) \quad (6)$$

Considering the results from Figures 5 and 6, Equations 7 and 8 are suggested to determine Lr/b and Wr/b on the basis of b/B and R respectively. r2 is the mean squares of the equation. θ and Fr have been assumed to be fixed amounts.

$$\frac{L_r}{b} = 3.575(\frac{b}{B})^{0.446} R^{\ 0.278} \qquad r^2 = 0.845 \quad (7)$$

$$\frac{W_r}{b} = 0.365(\frac{b}{B})^{0.415} R^{\ 0.296} \qquad r^2 = 0.895 \quad (8)$$

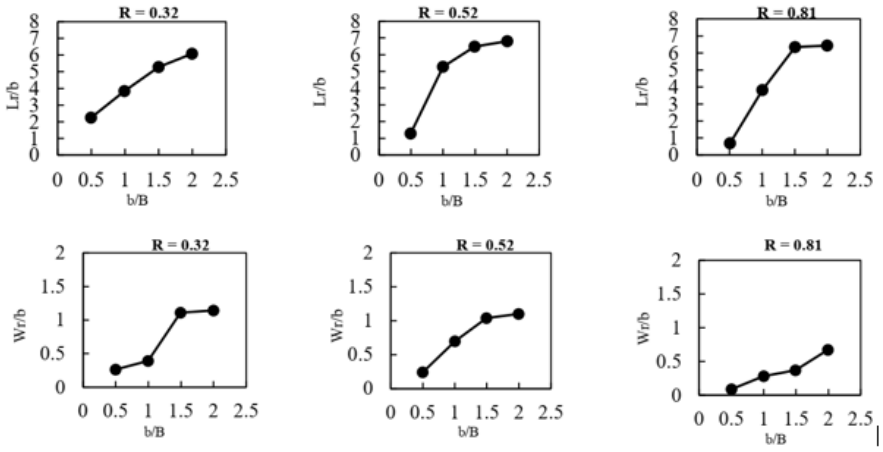

Fig 6. comparing W_r/b and L_r/b based on different b/B in different discharge distribution ratios

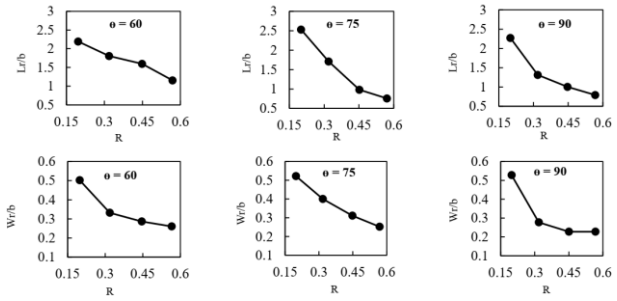

Fig7. the numerical results of W_r/b and L_r/b in terms of R in different intake angles

3.2. Studying the effects of intake angle and Froude number of the entering flow on the size of the separation zone flow

First the effects of four discharge distribution ratios (R) of 0.2, 0.32, 0.45 and 0.57 were studied in three intake angles of 60, 75 and 90 degrees for the constant Froude number equal to 0.3. Figure 7 has been illustrated for the dimensionless length and width of the separation zone of the flow in the numerical state through measuring the length (Lr) and the width (Wr) of the separation zone created in the intake.

As it can be seen in Figure 7 for each specific intake angle, as the dewatering discharge ratio increases the transverse component of velocity increases in front of the intake mouth and the length of the separation zone shortens within the intake and its wide becomes smaller as well. Equation 9 is obtained based on Equation 5 and deleting b/B and Fr since they are constant.

$$\frac{L_r}{b}, \frac{W_r}{b} = F(R, \theta) \quad (9)$$

Considering the results of Figure 7, Equations 10 and 11 are suggested for determining Lr/b and Wr/b respectively

in terms of R and θ. r2 is the mean squares of the equation and the angle is measured in radian.

$$\frac{L_r}{b} = 0.64(\theta)^{0.621} R^{0.742} \quad r^2 = 0.945 \tag{10}$$

$$\frac{W_r}{b} = 0.256(\theta)^{0.523} R^{0.813} \quad r^2 = 0.927 \tag{11}$$

Considering the outcome, Equations 12 and 13 are suggested for determining Lr/b and Wr/b respectively in terms of θ. r2 is the mean squares of the equation and the angle is also measured in radian. R, Fr and b/B have been considered to be constant in these Formulas.

$$\frac{L_r}{b} = 0.0022\theta^2 + 0.234\theta + 2.253 \quad r^2 = 0.852 \tag{12}$$

$$\frac{W_r}{b} = 0.0009\theta^2 + 0.28\theta + 0.486612 \quad r^2 = 0.822 \tag{13}$$

In order to investigate the effect of the entering flow Froude number on the size of the separation zone created in the intake, Figure 8 shows the dimensionless length and width of the flow's separation zone in terms of the Froude numbers of the flow 0.32 to 0.45 for the constant ratio of discharge distribution of 0.2 and 45 degrees constant intake angle.

Considering Figure 8, a change in the Froude number of the main channel slightly changes the length and the width of the separation zone in the intake channel's entrance which indicates the insignificant effects of these parameters on the size of the formed separation zone in it he mouth of the intake. Considering the results obtained from the numerical studies and the sum of the formulas resulted from them the general Equations 14 and 15 are suggested in this section for determining the dimensionless length and width of the separation zone created in the intake.

$$\frac{L_r}{b} = 2.52\left(\frac{b}{B}\right)^{0.399} Fr^{0.001} R^{0.412} \theta^{0.805} \quad r^2 = 0.812 \tag{14}$$

$$\frac{W_r}{b} = 0.239\left(\frac{b}{B}\right)^{0.702} Fr^{0.698} R^{0.376} \theta^{0.761} \quad r^2 = 0.798 \tag{15}$$

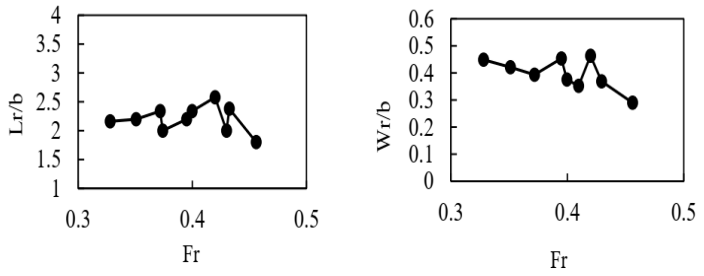

Fig 8. comparing the numerical results of Lr/b and Wr/b in terms of different Froude numbers of the entering flow in 45 degrees intake angle

4. Conclusion

Identifying the flow patterns where the intakes meet is of crucial importance. The separation zone leads to changes in the velocity distribution and the flow pattern in the confluence area. The sum of the obtained results from studying the hydraulic flow in this study includes: The effects of influential parameters such as the flow discharge ratio and different ratios of width on the separation zone size were studied numerically and compared with Kusthuri, Pundarikanthan's [14] experimental results and some numerical equations were also presented.After studying the effect of the flow's Froude number in the upstream of the main channel and the intake angle on the size of the separation zone, the numerical results showed that as the flow Froude number in the main channel changes, the length and the width of the separation zone change slightly in the entrance of the branch channel which indicates the insignificant effect of this parameter on the size of the separation zone created in the mount of the branch channel. General equations and also graphs which show changes in dimensionless length (Lr/b) and width (Wr/b) of the separation zone in terms of discharge distribution ratio of 0.32 to 0.57, intake angle of 45 to 90 degrees and the ratio of widths 1 and 2 for the constant Froude number of the entering flow were extracted taking into consideration the results obtained from CFX model and the sum of formulas obtained from them.

References

1. Taylor, E. 1944. "Flow characteristics at rectangular open channel junction, Journal of Hydraulic Engineering", 10(6), pp. 893-902.

2. Neary, VS., Odgaard, A. and Sotiropoulos, F. 1999. "Three-dimensional numerical model of lateral- intake inflows", Journal of Hydraulic Engineering, 125(2) , pp. 126-140.

3. Karimi S., Bonakdari H., and Gholami A. 2015. "Numerical examination of the effect of the location of flowmeters in intakes on flow velocity measurement accuracy". Special Issue of Bulletin of Environment, Pharmacology and life sciences 2015, 4(7).

4. Barkdoll, B.D., Hagen, B.L. and Odgaard, A.J. 1998. "Experimental comparison of dividing open- channel with duct flow in T-junction. Journal of Hydraulic Engineering", 124(1) , pp. 92-95.

5. Issa, R.I. and Oliveira, P.J. 1994. "Numerical prediction of phase separation in two-phase flow through T-junction", Comp. and Fluids, 23(2) pp., 347-356.

6. Neary, V.S. and Sotiropoulos, F. 1996. "Numerical investigation of laminar flows through 90-degree diversions of rectangular cross-sec-tion", Computational and Fluids, 25(2) , pp. 95-118.

7. Law, S.W. and Reynolds, A.J. 1966. "Dividing flow in an open channel, Journal of Hydraulic Division", 92(2), pp. 4730-4736.

8. Neary, V.S. and Odgaard, A.J. 1993. "Three-dimensional flow structure at open channel diversions". Journal of Hydraulic Engineering, 119(11), pp. 1224-1230.

9. Ramamurthy, A., Qu, J. and Vo D. 2007. "Numerical and experimental study of dividing open-channel flows, Journal of Hydraulic Engineering", 133(10), pp. 1135-1144.

10. Wilcox, D. C. 2000. "Turbulence modeling for CFD", 2nd Ed., DCW Industries, Inc.

11. Olsen, N.B.R. 2006. "A three-dimensional Numerical Model for Simulation of Sediment Movements in Water Intakes with Moltiblock Option, Department of Hydraulic and Environmental Engineering", The Norwegian University of Science and Technology.

12. Hager, W. H. 1992. "Discussion of 'Dividing flow in open channels" by A. S. Ramamurthy, D. M. Tran, and L. B. Carballada. J. Hydraul. Eng., 118(4), pp. 634–637.

13. Hsu, C. C., Tang, C. J., Lee, W. J. and Shieh, M. Y. 2002. "Subcritical 90° equal-width open-channel dividing flow", J. Hydraul.Eng, 128(7), pp. 716–720.

14. Kasthuri, B. and Pundarikanthan, N.V. 1984. Discussion on Separation Zone at open Channel Junction, Journal of Hydraulic Engineering, 113(4), pp. 543-548.